Acta Mechanica Sinica (2014) 30(2):153–160
DOI 10.1007/s10409-014-0030-0

RESEARCH PAPER

Effect of electric boundary conditions on crack propagation in ferroelectric ceramics

F.-X. Li · Y. Sun · R.K.N.D. Rajapakse

Received: 16 March 2013 / Revised: 22 October 2013 / Accepted: 11 November 2013

Abstract In this paper, the effect of electric boundary conditions on Mode I crack propagation in ferroelectric ceramics is studied by using both linear and nonlinear piezoelectric fracture mechanics. In linear analysis, impermeable cracks under open circuit and short circuit are analyzed using the Stroh formalism and a rescaling method. It is shown that the energy release rate in short circuit is larger than that in open circuit. In nonlinear analysis, permeable crack conditions are used and the nonlinear effect of domain switching near a crack tip is considered using an energy-based switching criterion proposed by Hwang et al. (Acta Metal. Mater., 1995). In open circuit, a large depolarization field induced by domain switching makes switching much more difficult than that in short circuit. Analysis shows that the energy release rate in short circuit is still larger than that in open circuit, and is also larger than the linear result. Consequently, whether using linear or nonlinear fracture analysis, a crack is found easier to propagate in short circuit than in open circuit, which is consistent with the experimental observations of Kounga Njiwa et al. (Eng. Fract. Mech., 2006).

Keywords Ferroelectric ceramics · Crack propagation · Energy release rate · Electric boundary conditions · Domain switching

The project was supported by the National Natural Science Foundation of China (11002002 and 11090331).

F.-X. Li (✉$_1$) · Y. Sun
State Key Laboratory for Turbulence
and Complex Systems, College of Engineering,
Peking University, 100871 Beijing, China
e-mail$_1$: lifaxin@pku.edu.cn

R.K.N.D. Rajapakse (✉$_2$)
Faculty of Applied Sciences, Simon Fraser University,
Burnaby, V5A 1S6, Canada
e-mail$_2$: rajaaks@sfu.ca

1 Introduction

Ferroelectric ceramics are increasingly used in modern industries for applications such as sensors, actuators, ultrasonic motors, etc, due to their peculiar electromechanical coupling properties, ultrafast response and compact size. However, these materials have two problems which hinder their full potential in applications: One is the nonlinearity at large electric fields or under high stress which results in domain switching; and the other is high brittleness with fracture toughness around 1 MPa $\sqrt{\text{m}}$. In the past decades, both linear and nonlinear fracture mechanics of ferroelectric ceramics have been extensively studied by scholars [1–6]. However, there still exist large discrepancies regarding the effect of applied electric field on fracture of piezoelectric materials [7–11]. Currently, the mechanism of crack propagation under general electromechanical loading remains an open question [12–14].

On the other hand, with the electromechanical coupling effect, the properties of ferroelectric ceramics are strongly dependent on electrical boundary conditions. It is well known that the linear elastic constant in open circuit, S_{33}^D, and that in short circuit, S_{33}^E, have the following relationship [15]

$$S_{33}^D = S_{33}^E(1 - K_{33}^2), \tag{1}$$

where K_{33} is the longitudinal electromechanical coupling coefficient, $K_{33} = d_{33}\Big/\sqrt{k_{33}^\sigma S_{33}^E}$, where d_{33} is the longitudinal piezoelectric coefficient, and k_{33}^σ the free dielectric coefficient.

The material thus seems "harder" in open circuit than in short circuit. The nonlinear properties have a similar tendency as reported previously by Berlincourt and Krueger [16] and recently by Li and Fang [17]. More recently, Kounga Njiwa et al. [18] reported that a crack is easier to propagate in a short-circuit, compact tension (CT) PZT specimen than that in an open-circuit sample. According to

our knowledge, so far there are no theoretical studies specially addressing the effect of electric boundary conditions on the fracture of piezoelectric/ferroelectric ceramics.

In this study, we theoretically examine the effect of electric boundary conditions on the crack propagation in a Mode I crack under pure mechanical loading. The mechanism of crack propagation under general electromechanical loading is not addressed here, as we think that problem can not be solved by theoretical analysis alone. In the analysis, we use both linear and nonlinear fracture mechanics for ferroelectric ceramics and take the energy release rate as the driving force for crack propagation. In linear analysis, we use the Stroh formalism [19, 20] and a rescaling method to calculate the field solutions and then the energy release rate (ERR). In nonlinear analysis, domain switching near a crack tip is taken into account and the excess released potential energy after domain switching is added to the total ERR for crack propagation. In both cases, it is found that the ERR in short circuit is obviously larger than that in open circuit, and crack propagation in the former is thus easier than that in the latter, which qualitatively agrees well with the experimental observations by Kounga Njiwa et al. [18].

2 Linear analysis for crack propagation

In linear analysis, we use the Stroh formalism [19, 20] to analyze an impermeable crack embedded in an infinite ferroelectric ceramics with the poling directions along axis-3, as shown in Fig. 1. In the analysis, we consider two different electric boundary conditions: One is the short circuit case with zero applied electric field, another is the open circuit case with zero applied electric displacement. Both the strain ERR and total ERR are calculated to address the crack propagation in short circuit and open circuit. Since there exist slight discrepancies in the exact expressions for the strain ERR and total ERR [8, 9, 21, 22] of plane problems, it is necessary to check these solutions again. As the Stroh formulism has been used by other researchers previously [2, 8], we present only the major steps of the formulation and key results in the following sections.

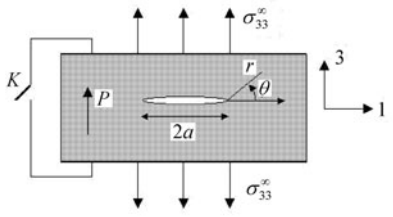

Fig. 1 Infinite piezoelectric plane containing a crack under remote tension in short circuit and open circuit

2.1 Formulation

The constitutive equations for piezoelectric materials can be written as [23]

$$\sigma_{ij} = c_{ijkl}u_{k,l} + e_{lij}\phi_{,l}, \quad D_i = e_{ikl}u_{k,l} - k_{il}\phi_{,l}, \tag{2}$$

where σ_{ij}, u_i, D_i, and ϕ are stresses, mechanical displacements, electric displacements, electric potential, respectively; and c_{ijkl}, e_{ijk}, k_{ij} are elastic constants, piezoelectric constants, and dielectric constants, respectively.

The strain, ε_{ij}, can be expressed by derivatives of mechanical displacements, u_i; and the electric field, E_i, by gradient of the electric potential, ϕ, as

$$\varepsilon_{ij} = \frac{1}{2}(u_{i,j} + u_{j,i}), \quad E_i = -\phi_{,i}. \tag{3}$$

For piezoelectric plan strain problems with the poling axis along x_3, assume field variables u_i and ϕ are functions of x_1 and x_3 only, i.e.,

$$u_k = A_k f(z), \quad \phi = A_4 f(z), \quad k = 1, 2, 3, \tag{4}$$

where $z = x_1 + px_3$.

Substituting Eq. (4) into Eqs. (2), we have

$$\begin{aligned} &c_{ijkl}A_k f_{,jl} + e_{lij}A_4 f_{,jl} = 0, \\ &e_{jkl}A_k f_{,jl} - k_{jl}A_4 f_{,jl} = 0, \\ &i, k = 1, 2, 3, \quad j, l = 1, 3. \end{aligned} \tag{5}$$

The above system of four homogeneous equations must be singular in order to yield nontrivial solutions for A_k (k = 1, 2, 3) and A_4, i.e.,

$$\begin{vmatrix} c_{i1k1} + (c_{i1k3} + c_{i3k1})p + c_{i3k3}p^2 & e_{1i1} + (e_{1i3} + e_{3i1})p + e_{3i3}p^2 \\ e_{1k1} + (e_{1k3} + e_{3k1})p + e_{3k3}p^2 & -[k_{11} + (k_{13} + k_{31})p + k_{33}p^2] \end{vmatrix} = 0. \tag{6}$$

For piezoelectric materials with the poling axis along x_3, using the reduced electromechanical coefficients, we have

$$\begin{vmatrix} c_{11} + c_{44}p^2 & 0 & (c_{13} + c_{44})p & (e_{15} + e_{31})p \\ 0 & c_{66} + c_{44}p^2 & 0 & 0 \\ \text{sym} & 0 & c_{44} + c_{33}p^2 & e_{15} + e_{33}p^2 \\ \text{sym} & 0 & \text{sym} & -(k_{11} + k_{33}p^2) \end{vmatrix} = 0. \tag{7}$$

Here the symbol "sym" in Eq. (7) denotes that the matrix is symmetric.

As the orders of the elastic constants, c_{ij} ($\sim 10^{10} - 10^{11}$ Pa), piezoelectric constants, e_{ij} ($\sim 10^0 - 10^1$ C/m^2), and dielectric constants, k_{ij} ($\sim 10^{-9} - 10^{-8}$ C/(V · m)) differ too much, we use a rescaling method [24] as follows to yield more accurate solutions to Eq. (7).

We rescale the units of relevant variables: force (GN); voltage (GV); stress, electric field and electric displacement to σ (GPa), E (GV/m), D (C/m^2), respectively; and the materials constants to $c_{ij} \sim 10^1$–10^2 GPa, $e_{ij} \sim 10^0$–10^1 C/m^2, $k_{ij} \sim 10^0$–10^1 C/(GV · m).

By solving Eq. (7), we can obtain eight eigenvalues, $p's$, forming four conjugate pairs, i.e., p_α, $\overline{p}_\alpha$, $\alpha = 1, 2, 3, 4$.

Then the displacements and electric potential can be expressed in terms of the eight eigenvalues as

$$v_m = \sum_{\alpha=1}^{4} A_{m\alpha} f_\alpha(z_\alpha) + \sum_{\alpha=1}^{4} \bar{A}_{m\alpha} \bar{f}_\alpha(\bar{z}_\alpha), \quad m = 1, 2, 3, 4, \tag{8}$$

where $\boldsymbol{v} = \begin{Bmatrix} u_k \\ \phi \end{Bmatrix}$, $\boldsymbol{A} = \begin{Bmatrix} A_{k\alpha} \\ A_{4\alpha} \end{Bmatrix}$, $k = 1, 2, 3$, $\alpha = 1, 2, 3, 4$, $z_\alpha = x_1 + p_\alpha x_3$, $\bar{z}_\alpha = x_1 + \bar{p}_\alpha x_3$.

Define new stress function χ and electric displacement function κ as

$$\sigma_{i1} = -\chi_{i,3}, \quad \sigma_{i3} = \chi_{i,1}, \quad D_1 = -\kappa_{,3}, \quad D_3 = \kappa_{,1}. \tag{9}$$

Then one can obtain the following relationships

$$\begin{aligned} \chi_i &= \sum_\alpha L_{i\alpha} f_\alpha(z_\alpha) + \sum_\alpha \bar{L}_{i\alpha} \bar{f}_\alpha(\bar{z}_\alpha), \\ \kappa &= \sum_\alpha W_\alpha f_\alpha(z_\alpha) + \sum_\alpha \bar{W}_\alpha \bar{f}_\alpha(\bar{z}_\alpha), \end{aligned} \tag{10}$$

where

$$L_{i\alpha} = (c_{i3k1} + p_\alpha c_{i3k3}) A_{k\alpha} + (e_{1i3} + p_\alpha e_{3i3}) A_{4\alpha}, \tag{11}$$

$$W_\alpha = (e_{3k1} + p_\alpha e_{3k3}) A_{k\alpha} - (k_{31} + p_\alpha k_{33}) A_{4\alpha}. \tag{12}$$

Then

$$\Phi_m = \sum_\alpha M_{m\alpha} f_\alpha(z_\alpha) + \sum_\alpha \bar{M}_{m\alpha} \bar{f}_\alpha(\bar{z}_\alpha), \quad m = 1, 2, 3, 4, \tag{13}$$

where $\boldsymbol{\Phi} = \begin{Bmatrix} \chi_i \\ \kappa \end{Bmatrix}$, $\boldsymbol{M} = \begin{Bmatrix} L_{i\alpha} \\ W_\alpha \end{Bmatrix}$, $i = 1, 2, 3$, $\alpha = 1, 2, 3, 4$.

The mechanical and electric surface conditions of an impermeable crack are

$$\sigma_{ij} n_j = 0, \quad D_i n_i = 0. \tag{14}$$

Following the derivations by Park and Sun [8], the general displacements can be obtained as

$$\begin{aligned} v_m = \frac{1}{2} \sum_\alpha \{ & A_{m\alpha} N_{\alpha n} [(z_\alpha^2 - 1)^{1/2} - z_\alpha] \\ & + \bar{A}_{m\alpha} \bar{N}_{\alpha n} [(\bar{z}_\alpha^2 - 1)^{1/2} - \bar{z}_\alpha] \} T_n, \end{aligned} \tag{15}$$

where $\boldsymbol{N}$ is the inverse matrix of $\boldsymbol{M}$ and $\boldsymbol{T}$ is the remote loading vector, i.e.,

$$\boldsymbol{T} = [\sigma_{13}^\infty, \sigma_{23}^\infty, \sigma_{33}^\infty, D_3^\infty]^{\mathrm{T}}. \tag{16}$$

The near tip field solutions can be obtained as follows when polar coordinates with their origins located at the center of the crack space (Fig. 1) are used. Then

$$z_\alpha = a + r(\cos\theta + p_\alpha \sin\theta), \tag{17}$$

and

$$\sigma_{k3} = \sqrt{\frac{a}{2r}} \mathrm{Re} \left\{ \sum_\alpha M_{k\alpha} \frac{1}{\sqrt{\cos\theta + p_\alpha \sin\theta}} N_{\alpha n} T_n \right\}, \quad k = 1, 2, 3, \tag{18a}$$

$$D_3 = \sqrt{\frac{a}{2r}} \mathrm{Re} \left\{ \sum_\alpha M_{4\alpha} \frac{1}{\sqrt{\cos\theta + p_\alpha \sin\theta}} N_{\alpha n} T_n \right\}. \tag{18b}$$

In previous studies, either the total energy release rate (ERR) [25, 26] or the mechanical strain ERR [8, 9] has been used as a fracture criterion for piezoelectric materials, both can be calculated by the crack closure integral [6, 7] as:

Total ERR

$$\begin{aligned} G_{\mathrm{I}}^{\mathrm{total}} &= J \\ &= \lim_{\delta \to 0} \frac{1}{\delta} \int_0^\delta (\sigma_{i3}(x) u_i(\delta - x) + D_i(x) \varphi(\delta - x)) \mathrm{d}x. \end{aligned} \tag{19}$$

Mechanical strain ERR

$$G_{\mathrm{I}}^{\mathrm{M}} = \lim_{\delta \to 0} \frac{1}{\delta} \int_0^\delta \sigma_{i3}(x) u_i(\delta - x) \mathrm{d}x. \tag{20}$$

2.2 Results

In this paper, PZT-4 piezoelectric ceramics is used for analysis and also for comparison with existing results [8, 9, 28]. The materials constants are listed in Table 1 using the rescaled units.

Table 1 Materials constants of PZT-4 ceramics using the rescaled units

Properties	Symbol	Value
Elastic stiffness constants	c_{11}^E/GPa	139
	c_{12}^E/GPa	77.8
	c_{13}^E/GPa	74.3
	c_{33}^E/GPa	113
	c_{44}^E/GPa	25.6
Piezoelectric constants	e_{31}/(C · m^{-2})	−6.98
	e_{33}/(C · m^{-2})	13.84
	e_{15}/(C · m^{-2})	13.44
Dielectric constants	k_{11}^ε/(C · (GV · m)$^{-1}$)	6.00
	k_{33}^ε/(C · (GV · m)$^{-1}$)	5.47

Note: $c_{66} = (c_{11} - c_{12})/2$

Using the above materials constants, the eigenvalues p_α are

$$p_\alpha = [1.191\,0\mathrm{i} \quad -0.274\,4 + 1.087\,1\mathrm{i} \quad 1.093\,3\mathrm{i} \quad 0.274\,4 + 1.087\,1\mathrm{i}], \quad \alpha = 1, 2, 3, 4. \tag{21}$$

The matrices $\boldsymbol{A}$ and $\boldsymbol{N}$ can then be obtained as

$$\boldsymbol{A} = \begin{bmatrix} 0.572\,2 & 0.496\,6 & 0 & -0.496\,6 \\ 0 & 0 & -0.577\,5 - 0.816\,4\mathrm{i} & 0 \\ 0.534\mathrm{i} & 0.206\,3 + 0.416\,5\mathrm{i} & 0 & 0.206\,3 - 0.416\,5\mathrm{i} \\ -0.622\,4\mathrm{i} & -0.318\,1 + 0.660\,5\mathrm{i} & 0 & -0.318\,1 - 0.660\,5\mathrm{i} \end{bmatrix}, \tag{22}$$

$$\boldsymbol{N} = \begin{bmatrix} -0.030\,1\mathrm{i} & -0.058\,1 - 0.000\,4\mathrm{i} & 0 & -0.058\,1 + 0.000\,4\mathrm{i} \\ 0 & 0 & 0.029\,2 + 0.020\,6\mathrm{i} & 0 \\ 0.053\,1 & -0.022\,9 - 0.064\,7\mathrm{i} & 0 & 0.022\,9 - 0.064\,7\mathrm{i} \\ -0.078\,8 & 0.026\,5 - 0.005\,3\mathrm{i} & 0 & -0.026\,5 - 0.005\,3\mathrm{i} \end{bmatrix}. \tag{23}$$

The total and strain energy release rate are

$$G_{\mathrm{I}}^{\mathrm{total}} = \frac{\pi a}{2}[1.74 \times 10^{-11}(\sigma_{33}^{\infty})^2 + 2 \times 2.22 \times 10^{-2}\sigma_{33}^{\infty}D_3^{\infty} - 8.74 \times 10^{7}(D_3^{\infty})^2], \tag{24}$$

$$G_{\mathrm{I}}^{\mathrm{M}} = \frac{\pi a}{2}[1.74 \times 10^{-11}(\sigma_{33}^{\infty})^2 + 2.22 \times 10^{-2}\sigma_{33}^{\infty}D_3^{\infty}]. \tag{25}$$

From Eqs. (24) and (25), it can be seen that in open circuit without applied electric displacement loading, the total ERR and the strain ERR are the same, which is easy to understand because in open circuit with merely applied stress, no electric energy is involved during crack propagation at all. It should be noted that the calculated strain ERR in Eq. (25) is the same as the result in the corrigenda by Sun and Park [22]. However, as the total ERR is not presented, a direct comparison is not possible.

As to the case of an applied electric field loading in short circuit, a remote electric field loading E_3^{∞} is equivalent to a remote electric displacement loading D_3^{∞} in open circuit as far as the field solutions and energy release rate are concerned (Fig. 2).

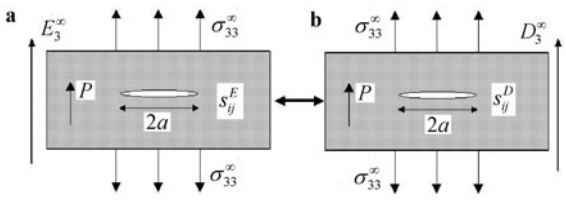

Fig. 2 Equivalent loading cases: **a** under remote applied electric field and **b** applied electric displacement

Therefore

$$D_3^{\infty} = d_{33}\sigma_{33}^{\infty} + k_{33}^{\sigma}E_3^{\infty}. \tag{26}$$

And equivalent strain

$$\varepsilon_{33(\mathrm{short})}^{\infty} = s_{33}^{E}\sigma_{33}^{\infty} + d_{33}E_3^{\infty}, \tag{27}$$

$$\varepsilon_{33(\mathrm{open})}^{\infty} = s_{33}^{D}\sigma_{33}^{\infty} + g_{33}D_3^{\infty} = (s_{33}^{D} + g_{33}d_{33})\sigma_{33}^{\infty} + g_{33}k_{33}^{\sigma}E_3^{\infty}. \tag{28}$$

Based on Eqs. (27) and (28), we have

$$s_{33}^{E} = s_{33}^{D} + g_{33}d_{33}, \quad d_{33} = g_{33}k_{33}^{\sigma}. \tag{29}$$

Note that Eq. (29) is obtained with slight approximation and is valid only for one-dimensional piezoelectric ceramics with its pole along axis-3.

By substituting Eq. (26) into Eqs. (24) and (25), using the materials constants, $d_{33} = 240\,\mathrm{pC/N}$, and $k_{33}^{\sigma} = 1 \times 10^{-8}\,\mathrm{C/(V \cdot m)}$ [8, 9], we get

$$G_{\mathrm{I}}^{\mathrm{total}} = \frac{\pi a}{2}(2.31 \times 10^{-11}(\sigma_{33}^{\infty})^2 + 2.5 \times 10^{-11}\sigma_{33}^{\infty}E_3^{\infty} - 8.74 \times 10^{-9}(E_3^{\infty})^2), \tag{30}$$

$$G_{\mathrm{I}}^{\mathrm{M}} = \frac{\pi a}{2}(2.27 \times 10^{-11}(\sigma_{33}^{\infty})^2 + 2.22 \times 10^{-10}\sigma_{33}^{\infty}E_3^{\infty}). \tag{31}$$

It can be seen from Eqs. (30) and (31) that in short circuit without electric field loading, the total ERR is slightly larger than the mechanical strain ERR. This is because during crack propagation in short circuit under remote tension, a small amount of electric energy is dissipated to thermal energies due to the piezoelectric effect. Also, it should be noted that the calculated strain ERR is the same as that by Sun and Park [22] and their accurate expression of the total ERR is not available.

By comparing Eqs. (24), (25) with Eqs. (30), (31), it can be seen that both the total ERR and the mechanical strain ERR in short circuit are larger than those in open circuit. Thus, for the linear piezoelectric fracture analysis, whether using the total ERR or strain ERR as the fracture criterion, a crack is easier to propagate in short circuit than in open circuit.

3 Nonlinear analysis for crack propagation

In the above linear analysis, domain switching is neglected during crack propagation. However in a real ferroelectric material, the singular stress or electric field near a crack tip may cause small-scale domain switching even when the remote loading is far below the coercive field [4]. In this section, we take into account domain switching near a crack tip using an energy based domain switching criterion [29]. Under pure mechanical loading, domain switching is caused by the applied stress and we use the permeable crack condition

to avoid electric field concentration near a crack tip. Furthermore, to simplify the calculation, we further assume that a ferroelectric material is both elastically and dielectrically isotropic.

The stress intense factor (SIF) for a Mode-I crack in infinite isotropic media is

$$K_{\mathrm{I}} = \sigma_{33}^{\infty}\sqrt{\pi a}. \tag{32}$$

Stress near the crack tip can be expressed as

$$\begin{Bmatrix}\sigma_{11}\\ \sigma_{22}\\ \sigma_{12}\end{Bmatrix} = \frac{K_{\mathrm{I}}}{\sqrt{2\pi r}}\cos(\theta/2)\begin{Bmatrix}1-\sin(\theta/2)\sin(3\theta/2)\\ 1+\sin(\theta/2)\sin(3\theta/2)\\ \sin(\theta/2)\cos(3\theta/2)\end{Bmatrix}. \tag{33}$$

Under pure mechanical loading, only 90° domain switching exists and the switching criterion of Hwang et al. [29] is

$$E_i\Delta P_i + \sigma_{ij}\Delta\gamma_{ij} \geqslant W_{90}. \tag{34}$$

In this paper, different from Hwang et al. [29], we use $W_{90} = \sqrt{2}P_0E_C$ to activate 90° and 180° switching simultaneously [30, 31].

To study the effect of domain switching on crack propagation, we consider the case of a domain with an original horizontal polarization, such as Domain 1 or Domain 2 in Fig. 3. Even in a vertically poled (along axis 3) ceramic as shown in Fig. 3, a considerable amount of such domains may still exist as a result of incomplete 90° domain switching [16, 31]. Let the volume fraction of the horizontal (or nearly horizontal) domains be f_{hor}, in a vertical poled ceramics. It is acceptable to assume $f_{\mathrm{hor}} \sim 5\% - 20\%$.

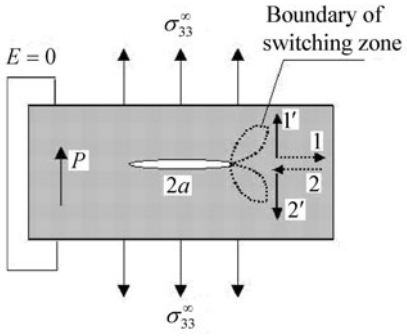

Fig. 3 Illustration of domain switching and switching zone under remote tension in short circuit

3.1 Domain switching in short circuit

In short circuit, the crack-tip domains 1 and 2 may switch to Domain 1′ and 2′, and no depolarization field is induced by domain switching in this way. Using Eqs. (33) and (34), the boundary of the 90° switching zone (Fig. 3) can be expressed in polar radius $r(\theta)$ as [4]

$$\sqrt{r} = \sqrt{R_{\mathrm{s}}}\sin\theta\sin(3\theta/2), \tag{35}$$

where R_{s} measure the size of the switching zone and can be expressed by

$$R_{\mathrm{s}} = \left(\frac{K_{\mathrm{I}}\gamma_{\mathrm{s}}}{2\sqrt{\pi}P_0E_C}\right)^2, \tag{36}$$

where γ_{s} is the magnitude of the spontaneous strain.

The area of the domain switching zone is

$$\begin{aligned}A_{\mathrm{short}} &= 2\int_0^{2\pi/3}\mathrm{d}\theta\int_0^{R_{\mathrm{s}}\sin^2\theta\sin^2(3\theta/2)} r\mathrm{d}r\\ &= \left(\frac{729\sqrt{3}}{8\,960}+\frac{3\pi}{32}\right)R_{\mathrm{s}}^2 = 0.44R_{\mathrm{s}}^2.\end{aligned} \tag{37}$$

To simplify the formulations, we use a moderate tension loading $\sigma_{33}^{\infty} = 15\,\mathrm{MPa}$ in the following derivations. The materials constants for PZT-4 ceramics are $\gamma_{\mathrm{s}} = 0.02$, $P_0 = 0.75\,\mathrm{C/m^2}$, $E_C = 1.0\,\mathrm{MV/m}$, $d_{33} = 289\,\mathrm{pC/N}$, $g_{33} = 26.1\,\mathrm{mV{\cdot}m/N}$, the isotropic Young's modulus $Y^E = 115\,\mathrm{GPa}$, $Y^D = 159\,\mathrm{GPa}$, the isotropic dielectric constant $k^{\sigma} = 11.5\,\mathrm{nC/(V\cdot m)}$. The size of the switching zone is thus calculated to be $R_{\mathrm{s}} = 0.04a$, where a is half of the crack length.

Under a constant applied stress loading, we assume that the stress field is unaffected by domain switching, in a way similar to that in the small scale yielding model in fracture mechanics. Such an assumption is acceptable since during domain switching strain (or displacement) along the loading direction increases and thus the applied stress does some positive work to the entire system. While in the case of a constant applied displacement loading, the strain (or displacement) along the loading direction is fixed during domain switching, and thus stress relaxes and the applied loading does not do any work. Under such an assumption, the excess released potential energy within the switching zone after domain switching is calculated as

$$\begin{aligned}W_{\mathrm{ex}}^{\mathrm{short}} &= 2f_{\mathrm{hor}}\cdot\int_0^{2\pi/3}\mathrm{d}\theta\int_0^{R_{\mathrm{s}}\sin^2\theta\sin^2(3\theta/2)}\left[\sin\theta\sin(3\theta/2)\right.\\ &\quad\left.\times\frac{K_{\mathrm{I}}\gamma_{\mathrm{s}}}{\sqrt{2\pi r}} - \sqrt{2}P_0E_C\right]r\mathrm{d}r\\ &= 0.463P_0E_Cf_{\mathrm{hor}}\times A_{\mathrm{short}}.\end{aligned} \tag{38}$$

The density of the excess released potential energy $\left[\sin\theta\sin(3\theta/2)\frac{K_{\mathrm{I}}\gamma_{\mathrm{s}}}{\sqrt{2\pi r}} - \sqrt{2}P_0E_C\right]$ is singular at the crack tip and gradually reduces to zero at the boundary of the domain switching zone. We assume that during crack propagation isotropic elasticity and dielectricity assumptions can be used, the total energy release rate consists of two parts, i.e.,

$$G_{\mathrm{iso}}^{\mathrm{total}} = G_{\mathrm{iso}}^{\mathrm{linear}} + G_{\mathrm{iso}}^{\mathrm{nonlinear}} = J_{\mathrm{I}}^{E} + \mathrm{d}W_{\mathrm{ex}}^{\mathrm{short}}/\mathrm{d}a, \tag{39}$$

where the crack tip closure J-integral relates to the SIF by

$$J_{\mathrm{I}}^{E} = \frac{1}{Y^E}K_{\mathrm{I}}^2. \tag{40}$$

The excess potential energy release rate $\mathrm{d}W_{\mathrm{ex}}^{\mathrm{short}}/\mathrm{d}a$ is

difficult to calculate, and here we use the upper limit to estimate it as

$$\mathrm{d}W_{\mathrm{ex}}^{\mathrm{short}}/\mathrm{d}a < 0.463P_0E_Cf_{\mathrm{hor}} \cdot \lim_{\Delta a\to 0} A_{\mathrm{shaded}}/\Delta a$$
$$= 0.463P_0E_Cf_{\mathrm{hor}} \times 0.78R_{\mathrm{s}}, \tag{41}$$

where A_{shaded} denotes the shaded area shown in Fig. 4.

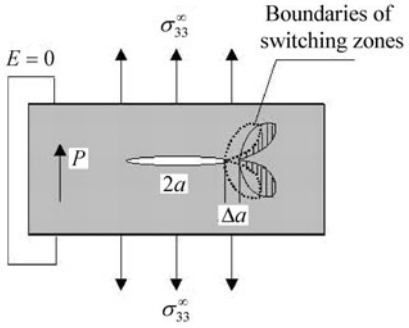

Fig. 4 Illustration of domain switching zone moving with crack propagation

3.2 Domain switching in open circuit

In open circuit with a remote tension σ_{33}^{∞}, the zero electric displacement loading is equivalent to a remote electric field loading as

$$E_3^{\infty} = -g_{33}\sigma_{33}^{\infty}. \tag{42}$$

With the existence of equivalent electric field loading E_3^{∞}, the switched Domains 1′ and 2′ tend to orient along the direction of E_3^{∞}, thus forming a large depolarization field in the switched domains. In the case in which Domains 1 and 2 completely switch to Domains 1′ and 2′, the depolarization field inside Domains 1′ and 2′ is

$$E_{\mathrm{d}} = P_0/k^{\sigma}, \tag{43}$$

where k^{σ} is the isotropic dielectric constant.

For a typical ferroelectric ceramic, E_{d} is about 10–100 times of the coercive field, thus usually Domains 1 and 2 can, not completely but partially, switch to Domains 1′ and 2′, which is represented by a volume fraction of β ($0 \leqslant \beta \leqslant 1$). The depolarization field is thus reduced to βE_{d} and the domain switching criterion can be rewritten as

$$(E_3^{\infty} - \beta E_{\mathrm{d}})P_0 + \sin\theta\sin(3\theta/2)\frac{K_{\mathrm{I}}\gamma_{\mathrm{s}}}{\sqrt{2\pi r}} = \sqrt{2}P_0E_C. \tag{44}$$

The shape of the switching zone in open circuit is the same as that in short circuit, but the size is different (see Fig. 5). In open circuit, the switching zone is split into two parts with the outer zone size R_1 and the inner zone size R_2 defined by

$$R_1 = \left(\frac{K_{\mathrm{I}}\gamma_{\mathrm{s}}}{2\sqrt{\pi}P_0E_C}\right)^2\left(1 - \frac{E_3}{\sqrt{2}E_C}\right)^{-2}, \tag{45}$$

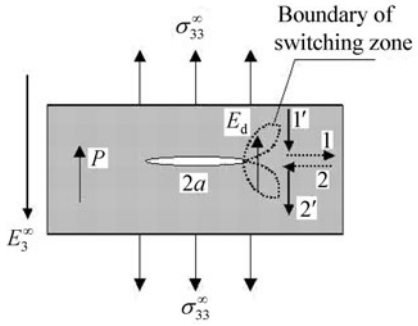

Fig. 5 Illustrations of domain switching and switching zone under remote tension in open circuit

$$R_2 = \left(\frac{K_{\mathrm{I}}\gamma_{\mathrm{s}}}{2\sqrt{\pi}P_0E_C}\right)^2\left(1 + \frac{E_{\mathrm{d}} - E_3}{\sqrt{2}E_C}\right)^{-2}. \tag{46}$$

In the inner zone $\sqrt{r} \leqslant \sqrt{R_2}\sin\theta\sin(3\theta/2)$, 90° domain switching can be completed as a result of the counteraction of the large stress field and depolarization field, and $\beta = 1$; In the outer zone $\sqrt{R_2}\sin\theta\sin(3\theta/2) < \sqrt{r} \leqslant \sqrt{R_1}\sin\theta\sin(3\theta/2)$, the 90° switching is not complete as the stress decreases, and $0 \leqslant \beta < 1$.

Under a typical loading of $\sigma_{33}^{\infty} = 15$ MPa, the equivalent remote electric field loading $E_3^{\infty} = -g_{33}\sigma_{33} = 0.392\,\mathrm{MV/m}$, $E_{\mathrm{d}} = 65.2\,\mathrm{MV/m}$, $R_1 = 1.91R_{\mathrm{s}} = 0.077a$, $R_2 \approx \dfrac{1}{2\,200}R_{\mathrm{s}}$.

The equivalent areas of the inner switching zone and the total switching zone are

$$A_{\mathrm{open}}^{\mathrm{in}} = 2\int_0^{2\pi/3}\mathrm{d}\theta\int_0^{R_2\sin^2\theta\sin^2(3\theta/2)} r\mathrm{d}r = 0.44R_2^2, \tag{47}$$

$$A_{\mathrm{open}}^{\mathrm{total}} = A_{\mathrm{open}}^{\mathrm{in}} + 2\beta\int_0^{2\pi/3}\mathrm{d}\theta\int_{R_2\sin^2\theta\sin^2(3\theta/2)}^{R_1\sin^2\theta\sin^2(3\theta/2)} r\mathrm{d}r$$
$$= 0.02 \times 0.44R_{\mathrm{s}}^2. \tag{48}$$

From Eqs. (37) and (48), it can be seen that although the total switching zone in open circuit is larger than that in short circuit, the equivalent area of switching zone is much smaller than that in short circuit as a result of the incomplete 90° switching in open circuit.

In the outer switching zone, all of the released potential energy is dissipated during domain switching, i.e., no excess released energy remains; while in the inner switching zone, the excess released potential energy after domain switching is

$$W_{\mathrm{ex}}^{\mathrm{open}} = 2f_{\mathrm{hor}}\int_0^{2\pi/3}\mathrm{d}\theta\int_0^{R_2\sin^2\theta\sin^2(3\theta/2)}\Big[\sin\theta\sin(3\theta/2)$$
$$\times\frac{K_{\mathrm{I}}\gamma_{\mathrm{s}}}{\sqrt{2\pi r}} - P_0(\sqrt{2}E_C + E_{\mathrm{d}} - E_3^{\infty})\Big]r\mathrm{d}r$$
$$= 21.4P_0E_Cf_{\mathrm{hor}} \times A_{\mathrm{open}}^{\mathrm{in}}. \tag{49}$$

Similar to that in short circuit, the upper limit of the excess potential energy release rate is

$$\mathrm{d}W_{\mathrm{ex}}^{\mathrm{open}}/\mathrm{d}a < 21.4P_0E_Cf_{\mathrm{hor}} \times 0.78R_2 = 9.7 \times 10^{-3}P_0E_Cf_{\mathrm{hor}} \times 0.78R_{\mathrm{s}}. \quad (50)$$

Then the total energy release rate is

$$G_{\mathrm{iso}}^{\mathrm{total}} = G_{\mathrm{iso}}^{\mathrm{linear}} + G_{\mathrm{iso}}^{\mathrm{nonlinear}} = J_{\mathrm{I}} + \mathrm{d}W_{\mathrm{ex}}^{\mathrm{open}}/\mathrm{d}a, \quad (51)$$

where $J_{\mathrm{I}}^{D} = \dfrac{1}{Y^{D}}K_{\mathrm{I}}^{2}$.

For a comparative study, Table 2 presents the comparison of energy release rates in a center-cracked PZT-4 ceramic subjected to typical remote tension loading of 15 MPa in short circuit and open circuit using both linear and nonlinear analysis. It can be seen that both in short circuit and in open circuit, the piezoelectric linear ERRs are about 30% larger than the isotropic linear ERR, which indicates that the isotropic assumption considerably underestimates the field concentration near a crack tip. In nonlinear analysis, using the typical $f_{\mathrm{hor}} = 10\%$, the ERR caused by domain switching is less than 20% of the linear ERR in short circuit and even less than 0.5% of the linear ERR in open circuit. Thus, domain switching has little effect on crack propagation in open circuit, while in short circuit it may significantly increase the linear ERR.

Table 2 Comparison of energy release rates in a center-cracked PZT-4 ceramic subjected to 15 MPa remote tension loading ($2a = 2$ mm)

Energy release rate	Linear piezoelectric fracture analysis		Isotropic, nonlinear analysis	
	Mechanical energy	Total energy	Linear part	Nonlinear part
	$G_{\mathrm{I}}^{\mathrm{M}}/(\mathrm{kPa}\cdot\mathrm{mm})$	$G_{\mathrm{I}}^{\mathrm{total}}/(\mathrm{kPa}\cdot\mathrm{mm})$	$G_{\mathrm{iso}}^{\mathrm{linear}}/(\mathrm{kPa}\cdot\mathrm{mm})$	$G_{\mathrm{iso}}^{\mathrm{nonlinear}}/(\mathrm{kPa}\cdot\mathrm{mm})$
Short circuit	8.02	8.16	6.14	$< f_{\mathrm{hor}} \cdot 10.8$
Open circuit	6.15	6.15	4.44	$< f_{\mathrm{hor}} \cdot 0.23$

4 Discussion

From the above analysis, it can be seen that whether linear or nonlinear model is used, the ERR in short circuit is always larger than that in open circuit. Crack is thus easier to propagate in short circuit than in open circuit. Although the crack geometry studied in this study is different from what was investigated by Kounga Njiwa et al. [18] recently (Note: the crack geometry in their experiment is three dimensional, thus difficult to analyze), we think these two cases are qualitatively similar and our theoretical results agree well with their experimental observations.

Another note is that in our analysis, the "open circuit" is an ideal open circuit which does not allow any charge leakage even under a rather high depolarization field. While in practice, charge leakage is inevitable under high voltage even in the case of a specimen immersed in a perfect insulating oil [17]. If the open circuit is realized by exposing the specimen to air and disconnecting the electrodes, charge leakage will be very serious because of the lower dielectric strength of the air. Unless the applied stress is very small (say 1 MPa), as far as strain or crack propagation is concerned, such an "open circuit" does not differ much from a short circuit [18].

It should also be reminded that in this work, interactions between the domain switching zone and the outer zone are neglected, just as in the small scale yielding model in fracture mechanics. However, in our recent experimental work [13, 14], it has been found that ferroelastic domain switching in ferroelectrics is always constrained by neighboring domains or grains, which is apt to break the sample. A fracture model taking into account the constrained domain switching is under consideration.

5 Conclusions

In summary, we studied Model I crack propagation in ferroelectric ceramics in short circuit and open circuit using both linear and nonlinear fracture mechanics. In linear analysis, we use the impermeable crack and calculate both the mechanical strain ERR and the total ERR. It is found that the two types of ERR are the same for pure stress loading in open circuit, while in short circuit, the total ERR is slightly larger because of the piezoelectric effect. In nonlinear analysis, we take into account the domain switching near a crack tip. The total energy release rate, which includes the linear J-integral and the excess potential energy release rate after domain switching, is taken as the fracture criterion. It shows that whether the linear or nonlinear analysis is used, the ERR in short circuit is always larger than that in open circuit. Crack is thus easier to propagate in short circuit than in open circuit, which accords well with recent experimental observations [18]. Finally, it is suggested that when the fracture of piezoelectric/ferroelectric materials is analyzed, special attention should be paid to the electric boundary conditions.

References

1 Parton, V.Z.: Fracture mechanics of piezoelectric materials. Acta Astronaut. **3**, 671–683 (1976)

2 Suo, Z., Kuo, C.M., Barnett, D.M., et al: Fracture mechanics for piezoelectric ceramics. J. Mech. Phys. Solids **40**, 739–765 (1992)

3 Gao, H., Barnett, D.M.: An invariance property of local energy release rate in a strip saturation model of piezoelectric fracture. Int. J. Fract. **79**, R25–R29 (1996)

4 Zhu, T., Yang, W.: Toughness variation of ferroelectrics by polarization switch under non-uniform electric field. Acta Mater. **45**, 4695–4702 (1997)
5 Xu, X.L., Rajapakse, R.K.N.D.: On a plane crack in piezoelectric solids. Int J Solids Struct **38**, 7643–7658 (2001)
6 Zhang, T.Y., Zhao, M.H., Tong, P.: Fracture of piezoelectric ceramics. Adv. Appl. Mech. **38**, 147–289 (2001)
7 Park, Y.E., Tobin, A.: On electric field effects in fracture of piezoelectric materials. In: Lee, J.S., Maugin, G.A., Shindo, Y. eds. ASME Mechanics of Electromagnetic Materials and Structures AMD-161, MD-42, 51–62 (1993)
8 Park, S.B., Sun, C.T.: Effect of electric field on fracture of piezoelectric ceramics. Int. J. Fract. **70**, 203–216 (1995a)
9 Park, S.B., Sun, C.T.: Fracture criteria for piezoelectric ceramics. J. Am. Ceram. Soc. **78**, 1475–1480 (1995b)
10 Wang, H., Singh, R.N.: Crack propagation in piezoelectric ceramics: Effect of applied electric field. J. Appl. Phys. **81**, 7471–7479 (1997)
11 Fu, R., Zhang, T.Y.: Effects of an electric field on the fracture toughness of poled lead zirconate titanate ceramics. J. Am. Ceram. Soc. **83**, 1215–1218 (2000)
12 Yan, D.J., Huang, H.Y., Cheung, C.W., et al.: Fracture criterion for conductive cracks in soda-lime glass under combined mechanical and electric loading. Int. J. Fract. **164**, 185–199 (2010)
13 Li, Y.W., Li, F.X.: Two-dimensional domain switching induced tensile fracture in a crack-free PZT ceramics under orthogonal electromechanical loading. Appl. Phys. Lett. **97**, 102903 (2010)
14 Li, Y.W., Li, F.X.: In situ observation of electric field induced crack propagation in $BaTiO_3$ crystals along the field direction. Scripta Materialia **67**, 601–604 (2012)
15 Jaffe, B., Cook, W.R., Jaffe, H.: Piezoelectric Ceramics. Academic Press, London and New York (1971)
16 Berlincourt, D., Krueger, H.H.A.: Domain processes in lead titanate zirconate and barium titanate ceramics. J. Appl. Phys. **30**, 1804–1810 (1959)
17 Li, F.X., Fang, D.N.: Effects of electrical boundary conditions and poling approaches on the mechanical depolarization behavior of PZT ceramics. Acta Mater. **53**, 2665–2673 (2005)
18 Kounga Njiwa, A.B., Fett, T., Lupascu, D.C., et al.: Effect of geometry and electrical boundary conditions on R-curve for lead zirconate titanate ceramics. Eng. Fract. Mech. **73**, 309–317 (2006)
19 Stroh, A.N.: Dislocations and cracks in anisotropic elasticity. Phil. Mag. **3**, 625–646 (1958)
20 Ting, T.C.T.: Anisotropic Elasticity: Theory and Applications. Oxford University Press, New York/Oxford, 134–163 (1996)
21 Kumar, S., Singh, R. N.: Comment on "Fracture criterion for piezoelectric ceramics". J. Am. Ceram. Soc. **79**, 1133–1135 (1996)
22 Sun, C.T., Park, S.B.: Reply to "Comment on 'Fracture criterion for piezoelectric ceramics' ". J. Am. Ceram. Soc. **79**, 1136 (1996)
23 Tiersten, H.F.: Linear Piezoelectric Plate Vibrations. Plenum Press, New York (1969)
24 Qi, H., Fang, D.N., Yao, Z.H.: FEM analysis of electromechanical coupling effect of piezoelectric materials. Comp. Mater. Sci. **8**, 283–290 (1997)
25 Park, Y.E.: Crack extension force in a piezoelectric materials. J Appl Mech-T ASME **57**, 647–653 (1990)
26 Sosa, H.: Plane problems in piezoelectric media with defects. Int. J. Solid Struct. **28**, 491–505 (1991)
27 Chen, Y.H., Lu, T.J.: Cracks and fracture in piezoelectrics. Adv. Appl. Mech. **39**, 121–215 (2002)
28 Balke, H., Drescher, J., Kommer, G.: Investigation of mechanical strain energy release rate with respect to fracture criterion for piezoelectric ceramics. Int. J. Fract. **89**, L59–L64 (1998)
29 Hwang, S.C., Lynch, C.S., McMeeking, R.M.: Ferroelectric/ferroelastic interactions and a polarization switching model. Acta Metall. Mater. **43**, 2073–2084 (1995)
30 Huber, J.E., Fleck, N.A., Landis, C.M., et al.: A constitutive model for ferroelectric polycrystals. J. Mech. Phys. Solids **47**, 1663–1697 (1999)
31 Li, F.X., Rajapakse, R.K.N.D.: A constrained domain switching model for polycrystalline ferroelectric ceramics. Part I: Model formulation and applications to tetragonal materials. Acta Mater. **55**, 6472–6480 (2007)